

Further Improving the Decoy State Quantum Key Distribution Protocol with Advantage Distillation

Walter O. Krawec

School of Computing
 University of Connecticut, Storrs CT USA
walter.krawec@uconn.edu

Abstract

In this paper, we revisit the application of classical advantage distillation (CAD) to the decoy-state BB84 protocol. Prior work has shown that CAD can greatly improve maximal distances and noise tolerances of the practical decoy state protocol. However, past work in deriving key-rate bounds for this protocol with CAD have assumed a trivial bound on the quantum entropy, whenever Alice sends a vacuum state in a CAD block (i.e., the entropy of such blocks is taken to be zero). Since such rounds contribute, negatively, to the error correction leakage, this results in a correct, though sub-optimal bound. Here, we derive a new proof of security for CAD applied to the decoy state BB84 protocol, computing a bound on Eve’s uncertainty in all possible single and vacuum photon events. We use this to derive a new asymptotic key-rate bound which, we show, outperforms prior work, allowing for increased distances and noise tolerances.

1 Introduction

Quantum key distribution (QKD) allows for the establishment of a shared secret key between two parties, Alice and Bob, which is secure against a computationally unbounded adversary Eve. This task is impossible to achieve classically, where some form of computational assumption is always required. QKD protocol design, and security proof methodologies, are by now a very rich and vast domain; for a general survey, the reader is referred to [1]. Nonetheless, there are still improvements that can be made to increase performance. These improvements can appear in more sophisticated hardware developments; they can also appear through new theoretical advances, either in protocol design, or through alternative security proof techniques producing more optimal secret key rate bounds. It is the latter that we focus on, in this paper.

Perhaps one of the most commonly used QKD protocol is the BB84 protocol [2] which involves Alice sending qubit states chosen randomly from two (or three) mutually unbiased bases. The receiving party measures the sent qubit in a randomly chosen basis; if the basis choices are identical, then parties should expect a correlated bit, otherwise the data is random and the round is discarded. In practice, Alice utilizes a weak coherent source to prepare her qubits. Such a source will prepare n photons with Poisson distribution $p(n|\mu)$, where μ is the mean photon number as determined by Alice’s device. When the source sends a single photon (i.e., $n = 1$), then that round is the “ideal” BB84 protocol, with single-qubit sources. However, when Alice sends two or more photons, Eve may perform a so-called photon number splitting (PNS) attack to learn all information on that

round [3, 4]. Of course, if Alice sends no photons, then Eve can learn nothing, however Bob also has no information to gain; Alice’s bit in this case is uniform random and independent of all parties.

Multi-photon events are devastating to QKD security as they completely destroy any hope of distilling a secure bit for that particular round. Thus, the power level μ should be kept “low” to avoid sending double photons. However, this increases the probability of sending no photons, thus limiting the overall effectiveness of the protocol. Another challenge when analyzing QKD under practical sources, is that, in order to bound the quantum entropy of the single-photon events, one requires knowledge of the single-photon error rate (i.e., the error induced by Eve’s attack conditioned on Alice sending a single photon) [5]. However, parties can only measure the *average* error across all photon numbers n .

To overcome the above challenges, the decoy state method was developed [6, 7, 8]. This method takes the standard BB84 protocol and allows Alice to alter the power level μ , randomly, every round. Since Eve cannot know the chosen power level, she cannot change her attack strategy across different power levels. This allows Alice and Bob to gain highly accurate knowledge of the single photon error rate, along with the probability of Alice and Bob distilling a raw key bit for each photon number. Ultimately, this knowledge, combined with the GLLP formula [5], allows for drastically improved key-rates (in particular, improved maximal distances between parties) for the BB84 protocol with practical devices.

While the decoy state method improves the performance of BB84 in practical scenarios, it is known that *classical advantage distillation* (CAD) methods [9] can improve the noise tolerance of QKD protocols in the ideal, single qubit scenario (see, for instance, [10]). Recently, CAD has been applied successfully to the decoy state protocol [11] showing that it can substantially improve maximal distances and noise tolerances of *practical* QKD implementations. Their results have also been used in a recent experimental implementation [12], showing improved performance through the use of CAD is possible, both theoretically, and now experimentally. CAD has also been applied recently to measurement device independent (MDI) QKD [11], twin-field QKD [13, 14, 15], conference key agreement protocols [16], and phase matching QKD [17]; in all cases it has been shown to improve performance under certain conditions (specifically, long distance or high noise scenarios).

CAD operates after the quantum communication stage of a QKD protocol finishes. In particular, quantum communication will first be used to establish a *raw key* which is a string of partially correlated, partially secret, key bits. CAD (discussed more in Section 1.1), works by dividing the raw key into blocks of size C , where C is set by the user. For each block, CAD will perform a two-way classical communication process, whereby, at the end, Alice and Bob will either distill a new raw key bit, or they will discard the block. Note that, at best, these C original raw key bits will result in only one new raw key bit, thus the new raw key will be *no larger* than $1/C$ of the original. However, it will hold that the new raw key will be more highly correlated. More details on the exact protocol are given in Section 1.1.

While CAD can produce a more correlated key, the two-way classical communication, which is done over the authenticated classical channel, necessarily leaks additional information to Eve. Thus, CAD can actually be detrimental to performance sometimes. However, it can be shown that if the noise in the channel is high, or if the distances between parties is large, CAD can be highly beneficial [11].

Note that when considering practical devices, a block of C raw key bits may have been produced by a combination of vacuum, single, and multi photon events (i.e., events where Alice initially sent

none, one, or many, photons respectively). It is not difficult to see (and we comment more on this later), that if a block of size C contains one or more multi photon events, that block is completely insecure and we must assume Eve knows everything on the final distilled bit. Thus, only blocks where all C rounds consist of vacuum or single photon events can potentially contribute towards Eve's uncertainty (and thus a non-zero secret key size). However, in all prior work we are aware of, involving CAD applied to the decoy state BB84 protocol, only blocks where all C rounds consist of single photon events were considered, while blocks with even a single vacuum round were neglected from the entropy computation, when computing Eve's uncertainty (which is needed to compute a key-rate bound as we discuss later in Section 1.1). Since these blocks do contribute negatively to the total error correction leakage, this leads to a potential sub-optimal result.

In this paper, we revisit a standard CAD protocol from [10] (modified from [9]), and apply it to the decoy state protocol, computing an asymptotic key-rate bound. Our new bound involves all possible blocks consisting of single and vacuum events. Since blocks involving multi-photon events are insecure, our result is optimal in this sense. To our knowledge we are the first to consider all such events when analyzing CAD with practical devices and the decoy state BB84 protocol. We compare with prior work in [11] and show that our result allows for increased distances and noise tolerances. We also evaluate both the infinite decoy state (which was considered in [11]), and also the more practical two decoy state protocol [18]. Again, here, we show our result performs better than prior work.

Our main result is a bound on the entropy of any block consisting of n single photon events and m vacuum events, with $m + n = C$, and is stated in Theorem 2. We use this to derive a key-rate result (Equation 57). At a high level, our result states that one may bound the entropy of a block of C bits, after CAD is applied, by considering all possible combinations of vacuum and single photon events, with the number of such events summing to C , the CAD block size. In particular, we show that the key-rate is lower bounded by r , where:

$$r \propto \left(\sum_{n=0}^C \binom{C}{n} G_1^n G_0^{C-n} \frac{Q_1^n + (1 - Q_1)^c}{2^{C-n}} f(n, Q_1) \right) - \mathbf{leak}_{EC}. \quad (1)$$

Above, G_j is the probability that Alice sent j photons on a round, conditioned on Alice and Bob distilling a raw key bit; Q_1 is the single-photon error rate; $f(n, Q_1)$ is a function we derive in Theorem 2, to compute Eve's uncertainty when there were n single photons in a C -bit block (and $m = C - n$ vacuum events in the block); and \mathbf{leak}_{EC} is the error correction leakage. The values of G_j and Q_1 can be estimated using the decoy state method.

While our result is an asymptotic key-rate result, our work can be used to analyze the finite key scenario by taking advantage of certain approximation methods (which we comment on later). However, while this will provide a security proof in the finite key case, it will be sub-optimal. Analyzing finite key bounds through more direct measures would be exciting future work. As we are solely interested in understanding the theoretical capabilities of CAD applied to the decoy state protocol, and to show, for the first time, that blocks with vacuum events can be handled in the security proof, we consider a tight finite key proof to be out of scope of this paper. Interestingly, as we were writing this, [19] derived a finite-key result for the decoy state protocol, but with a different CAD protocol than the one we consider here (or the one considered originally in [11]). Their CAD protocol involved Bob sending more information than he does with the protocol we work with, here. Because of this, the protocol they considered was claimed to be insecure on blocks containing vacuum rounds, and so those were not evaluated in their security proof either. In this work, we

show that, for the original CAD protocol considered in [11], blocks with vacuum rounds can be used in the security proof and lead to non-zero entropy. Future work, combining proof techniques from [19] with our methods in this paper, may prove fruitful in designing a more direct finite key bound for the standard CAD protocol and decoy state BB84. We leave that as interesting future work.

Ultimately, our work shows that further improved distances and noise tolerances are possible for the standard decoy state BB84 protocol, when augmented by CAD. Prior work [11] showed that CAD can substantially improve performance; we augment their results by deriving an alternative proof of security that is capable of producing a more optimistic bound on the conditional entropy of the system (needed to compute the key-rate of a QKD protocol [20, 21]). Our proof method may have independent interest for other CAD style protocol proofs. Finally, we evaluate our new result and compare to prior work, in a variety of settings, both for the four state and the six state BB84. We also consider both the infinite decoy state method and the more practical two-decoy method [18]. Taken as a whole, our work shows that there are still improvements to be discovered in standard QKD protocols; our work also further enhances our understanding of how classical post-processing methods, such as CAD, can greatly benefit quantum systems.

1.1 Preliminaries

We now discuss some basic notation and technical results that will be required later. Given a pure quantum state $|\psi\rangle$, we write $[\psi]$ to mean $|\psi\rangle\langle\psi|$. Given a density operator ρ_{AB} acting on some Hilbert space $\mathcal{H}_A \otimes \mathcal{H}_B$, we write ρ_B to mean $\rho_B = \text{tr}_A \rho_{AB}$. Finally, we say a state ρ_{AB} is a classical-quantum state (or cq-state) if it may be written $\rho_{AB} = \sum_a p_a [a]_A \otimes \rho_B^{(a)}$. We also say such a state is *classical on A*. Given a state $\rho_{AB} = \sum_x p_x \rho_{AB}^{(x)}$, which is classical on A , it is easy to verify that $H(A|B)_\rho \geq \sum_x p_x H(A|B)_{\rho^{(x)}}$.

A *double CNOT* (*DCNOT*) operator, is a unitary operation controlled on two qubits, c_1 and c_2 , with a third target qubit, t . Its action is to apply two sequential CNOT operations: the first controlled on c_1 , the second controlled on c_2 , with both CNOTs targeting t . Given a basis state $|a, b, c\rangle_{c_1 c_2 t}$, its action on such a state is simply: $\text{DCNOT} |a, b, c\rangle_{c_1 c_2 t} = |a, b, c \oplus a \oplus b\rangle_{c_1, c_2, t}$.

We denote the Bell basis states, by $|\phi_x^y\rangle$, where $x, y \in \{0, 1\}$. These are defined to be:

$$|\phi_x^y\rangle = \frac{1}{\sqrt{2}} |0, x\rangle + (-1)^y \frac{1}{\sqrt{2}} |1, \bar{x}\rangle = \frac{1}{\sqrt{2}} \sum_{a=0}^1 (-1)^{a \cdot y} |a, a \oplus x\rangle, \quad (2)$$

where $\bar{x} = 1 - x$ and $a \cdot y$ is standard multiplication.

Let X be a classical random variable, then we write $H(X)$ to mean the Shannon entropy of X . If X takes value x with probability p_x , then $H(X) = -\sum_x p_x \log_2 p_x$. The conditional Shannon entropy is denoted $H(X|Y)$ and is defined to be $H(X|Y) = H(XY) - H(Y)$. Finally, we denote by $h(x)$, for $x \in [0, 1]$, to be the binary Shannon entropy function, namely $h(x) = -x \log_2 x - (1 - x) \log_2(1 - x)$.

Given ρ_{XY} , a density operator, then we write $H(XY)_\rho$ to mean the von Neumann entropy of ρ_{XY} . If the context is clear, we may forgo writing the subscript. This is defined to be $H(XY)_\rho = -\text{tr}(\rho_{XY} \log_2 \rho_{XY})$. The conditional von Neumann entropy is denoted $H(X|Y)_\rho$ and defined to be $H(X|Y)_\rho = H(XY)_\rho - H(Y)_\rho$, where $H(Y)_\rho$ is the von Neumann entropy of $\rho_Y = \text{tr}_X \rho_{XY}$. Note that on classical systems, von Neumann entropy and Shannon entropy agree, thus we use the same notation for both, as is typical in quantum information theory.

The following theorem from [22] will be useful later:

Theorem 1. (From [22]): Let ρ_{AE} be classical on A such that:

$$\rho_{AE} = \frac{1}{N} [0]_A \otimes \left(\sum_{i=0}^M [E_i^0]_E \right) + \frac{1}{N} [1]_A \otimes \left(\sum_{i=0}^M [E_i^1]_E \right), \quad (3)$$

where the states $|E_i^k\rangle$ are not necessarily normalized, nor orthogonal. Then, it holds that:

$$H(A|E)_\rho \geq \frac{1}{N} \sum_{i=0}^M (\langle E_i^0 | E_i^0 \rangle + \langle E_i^1 | E_i^1 \rangle) \times \left(h \left[\frac{\langle E_i^0 | E_i^0 \rangle}{\langle E_i^0 | E_i^0 \rangle + \langle E_i^1 | E_i^1 \rangle} \right] - h[\lambda_i] \right), \quad (4)$$

where:

$$\lambda_i = \frac{1}{2} \left(1 + \frac{\sqrt{(\langle E_i^0 | E_i^0 \rangle - \langle E_i^1 | E_i^1 \rangle)^2 + 4Re^2 \langle E_i^0 | E_i^1 \rangle}}{\langle E_i^0 | E_i^0 \rangle + \langle E_i^1 | E_i^1 \rangle} \right) \quad (5)$$

Classical Advantage Distillation (CAD): Classical advantage distillation (CAD) is a purely classical process, introduced in [9], which takes as input two classical strings A and B , and outputs two new classical strings \tilde{A} , and \tilde{B} , such that the output strings are smaller, but have fewer expected bit errors. While there are several CAD protocols, we consider a version from [10] (also the one considered in [11]). Here, the original input strings are divided into *blocks* of C bits each, where $C \geq 2$ is specified by the user and is public knowledge. We then set \tilde{A} and \tilde{B} to initially be the empty string.

For each block, let $a_1 a_2 \cdots a_C$ be the C bits from A and $b_1 b_2 \cdots b_C$ be the C bits from B . The holder of A (who we will assume is Alice), will choose a *single* uniform random bit k for this block. She will then send to Bob (the holder of B), using an authenticated classical channel, the message $p_1 p_2 \cdots p_C$, where $p_i = a_i \oplus k$. That is, she will XOR each of her C bits with the same, randomly chosen, k . We use “ p ” to denote the message as it is “public” in the sense that an adversary, who may hold some information on A and B , now also holds this additional information stored in p .

Now, the message $p_1 \cdots p_C$ is received by Bob who will XOR this message with his C bit block, resulting in $x_1 x_2 \cdots x_C$, where $x_i = p_i \oplus b_i$. If $x_1 = x_2 = \cdots = x_C$ (i.e., if all C bits of this XOR computation are either zero or all one), then Bob will signal to Alice to “accept” this block; otherwise he will signal to “reject” this particular block. Note that this is also done over the authenticated channel and that CAD requires this “two way” communication.

If the block is rejected, all C bits from A and B are discarded and no additional bit is added to \tilde{A} or \tilde{B} . If the block is accepted, then Alice will add k to \tilde{A} while Bob will add x_1 to \tilde{A} (note that $x_1 = x_2 = \cdots = x_C$). In this case, the original C bits from A and B are also discarded. The process repeats the above, with Alice choosing a new k , independently of the last round, for the next C bits.

Note that, if a block is accepted, C bits are discarded, while only one is added. Furthermore, a bit is only added if the users accept a block. Let p_a be the probability of accepting a block, then the expected size of the new raw key is $|\tilde{A}| = p_a |A|/C$. That is, the new raw key will be smaller, perhaps substantially so, if C is large, or p_a is small. However, let’s consider the bit error in the new raw key.

It is clear to see that, if there are no errors at all between the original strings A and B (where an error is considered to be a bit in B that is not equal to the corresponding bit in A), then there

will be no errors between \tilde{A} and \tilde{B} . On the other hand, if the probability of a bit flip error between A and B is Q , then after running CAD, the expected error will be $Q^C/(Q^C + (1 - Q)^C)$. This is due to the fact that, the only way for an error to occur in the new strings, is if *all* of Bob's C bits in a particular round are errors, which occurs with probability Q^C . Of course, we must also condition on accepting a round, and the probability of accepting is $p_a = Q^C + (1 - Q)^C$, since Bob will signal to accept only if all his C bits are the same or if they are all flipped. More details can be found in [9, 10].

QKD Security: A QKD protocol typically involves two stages: a *quantum communication stage*, followed by a *classical post processing stage*. The former utilizes a quantum channel, along with an authenticated classical channel, over multiple *rounds*, to establish a *raw key*. This raw key is partially correlated and partially secret and thus is not suitable for immediate use as a secret key. The second stage is purely classical and, utilizing the authenticated channel, will take the raw keys and output a final secret key. The classical post processing stage consists, at a minimum, of an error correction protocol and a privacy amplification protocol. However, it may also consist of additional sub-routines, such as classical advantage distillation (CAD), or even noisy post processing [20], all of which are typically run before error correction and privacy amplification.

Of importance is the *key rate* of a QKD protocol. Let N be the total number of rounds performed in the quantum communication stage, and let ρ_{ABE} be the state representing Alice and Bob's raw key registers, before error correction and privacy amplification are run (though after any additional processing, such as CAD). We assume the A and B registers are classical on n -bits (with, of course, $n \leq N$), while Eve's system is arbitrary. Let ℓ be the resulting size, in bits, of the final secret key after privacy amplification is run (we have $\ell \leq n \leq N$). Then, the key rate of the QKD protocol is defined to be the ratio ℓ/N ; in the asymptotic scenario, we take $N \rightarrow \infty$.

Under the assumption of *collective attacks*, whereby Eve performs the same, potentially probabilistic, attack every round of the protocol, but is permitted to postpone measuring her ancilla until any future point in time, the state ρ_{ABE} takes the form $\rho_{ABE}^{\otimes n}$. In this case, it was shown in [20, 21], that:

$$\lim_{n \rightarrow \infty} \frac{\ell}{n} = H(A|E)_\rho - H(A|B)_\rho, \quad (6)$$

where the above entropies are computed on a single round of the system. Assuming $n = pN$, for some fixed constant p , then this can be used to compute a bound on the key rate ℓ/N for $N \rightarrow \infty$.

2 Decoy State BB84

We recall, first, the standard decoy-state BB84 protocol [6, 7, 8]. Our description will be high level, leaving the reader to refer to [6, 7, 8] for additional details on the protocol itself. The protocol operates assuming Alice utilizes a weak-coherent source which emits n photons according to Poisson distribution $p(n|\mu)$, where μ is the mean photon number, which may be set by Alice. Here:

$$p(n|\mu) = \frac{\mu^n}{n!} e^{-\mu}. \quad (7)$$

The protocol operates similar to the standard BB84 protocol [2], but with the additional feature that Alice will choose random power levels each round. In particular, let M be a set of available power levels to choose from, where $M = \{\mu, \nu_1, \nu_2, \dots\}$. Here, μ is a distinguished power level that

will be used for distilling raw key bits (called the *signal state power level*), while the other ν_i are *decoy power levels*. M may be infinite or finite (in practice, $|M|$ is typically two or three [18]).

The quantum communication stage of the protocol consists of N rounds, for N sufficiently large. On any particular round, the following process occurs:

1. Source:

- Alice chooses a random power level $\nu \in M$. The specific choice of power level for this round is kept secret for now. Note that the distribution over power level choices need not be uniform; asymptotically, we may set the probability of choosing μ , the signal state level, to be arbitrarily close to one.
- Alice next chooses a random key-bit k and a random basis X or Z . She emits a pulse from her source using her chosen power level ν , encoding the state k , in the chosen basis. Similar to above, the basis choice distribution need not be uniform, and we may bias towards the Z basis.

2. Receiver:

- The receiver, Bob, will choose a random basis to measure in, either the Z or X basis. His measurement produces one of four possible outcomes: ‘vacuum’ (he did not detect anything), ‘0’ (the zero state of the measured basis, e.g., $|0\rangle$ or $|+\rangle$); ‘1’ (the one state); or ‘double’ (his measurement produced a double-click, namely both 0 and 1).

3. Sifting:

- Alice and Bob disclose their basis choice. If they are not equal, the round is discarded.
- If (1) Alice and Bob both chose the Z basis; (2) Bob did not observe a vacuum (so he either observed zero, one, or double); and (3) if Alice chose $\nu = \mu$ (the signal state power level), then this round will contribute towards Alice and Bob’s *raw key*. In particular, Alice will use k for her raw key bit, while Bob will use his measurement outcome. If Bob observed a double click, he will choose a random bit for his raw key bit.
- If Alice and Bob both chose the X basis, or if Alice chose $\nu \neq \mu$, Alice will disclose her choice of k and Bob will disclose his measurement outcome. This will allow Alice and Bob to estimate the noise in the channel.

Note that the Sifting stage, above, can be performed after all N rounds of the quantum communication stage have been completed. Alice and Bob will also disclose a random subset of their raw key in order to estimate the error in their Z basis measurements for power level μ . Note, also, that the six-state BB84 protocol is identical to the above, however a third basis, the Y basis, is also added.

The above allows parties to observe several quantities. In particular, they may estimate the *gain* and the *noise* for each power level, individually. They may also estimate the noise in each basis and each power level combination. What parties cannot directly estimate is the noise or the gain, conditioned on Alice initially sending n photons. However, by modifying the power level randomly, one may get very tight bounds on these quantities. We will discuss this in more detail, in Section 3.3.

Following the completion of the above quantum communication stage, Alice and Bob each hold raw keys A and B . They will then run the CAD process, discussed in the previous section, to distill

new raw keys \tilde{A} and \tilde{B} . From this, they will then run error correction and privacy amplification, to yield their final, secret, key.

When CAD is run on a practical implementation of QKD, one must take into account that raw key bits may be distilled from vacuum events (when Alice sent nothing, but Bob's detector clicked), or when Alice sent multiple photons. Consider a block of C raw key bits and recall the operation of CAD, discussed earlier. If just one of the raw key bits in that block was distilled from an event where Alice sent two or more photons, it is straight forward to see that Eve will learn everything about the new raw key bit distilled from the CAD process. Since Eve, in theory, will know Alice's raw key bit for the round where she initially sent two or more photons, when Alice reveals her public message from the CAD process, Eve can easily determine the new choice of k for this block. Thus, only blocks of C raw key bits where all C rounds consist of vacuum and single photon events can possibly lead to a secure key bit after CAD runs. Any block with one or more multi-photon events, cannot contribute to Eve's uncertainty.

3 Security Analysis

We now compute a secret key rate for the CAD protocol, where some blocks contain a mix of vacuum and single photon events. Note that, by vacuum and single photon events or rounds, we mean those rounds where Alice sent zero or one photons respectively, *and* where Bob's detectors click and so he distills a raw key bit. We will do this by first tracing out the execution of the CAD process on a single block of C rounds, consisting of a mixture of m vacuum rounds and n single photon rounds (where $m + n = C$). This will allow us to compute a bound on the von Neumann entropy of such a block. Finally, we will use this result to analyze the entire protocol.

Note that, in the following, we distinguish between *rounds* and *blocks*. Rounds are individual quantum communication rounds used by the decoy state protocol, to distill the initial raw key (*before* CAD runs). A block is a sequence of C original raw key bits, used by the CAD process. Note that not all rounds lead to a raw key bit; however all raw key bits are organized into blocks.

3.1 Conditional Entropy in a Single Block

We will first consider a block of C raw key bits, m of which were distilled when Alice sent a vacuum, while n were distilled when Alice sent a single photon. Of course, we have $n + m = C$. Whenever Alice sends two or more photons on a round, that entire block is potentially compromised, so we do not analyze those cases and, later, will simply set the von Neumann entropy to zero for such events. In this section we will assume Eve employs a collective attack strategy; thus, while her attack may be a probabilistic process and depend on the photon number leaving Alice's lab initially, Eve will perform the same strategy across each round of the protocol. Later, we will show how this can be promoted to security against general attacks.

When Alice sends a vacuum state, normally Bob will only detect a photon through dark count events. However, since Eve is able to influence the channel arbitrarily, Eve may send any arbitrary state to Bob in this event. However, importantly, Alice's raw key bit is completely separate from Bob and Eve in such case as no information leaves Alice's lab. Thus, a vacuum round results in a joint state of the form:

$$\rho_{ABE}^{(vac)} = \frac{I_A}{2} \otimes \rho_{BE}, \quad (8)$$

where ρ_{BE} is some arbitrary state where the B register consists of a qubit, potentially entangled with Eve, and I_A is the completely mixed qubit state. We may assume ρ_{BE} is a pure state (otherwise, we may purify it and give the purification to Eve). Thus:

$$\rho_{ABE}^{(vac)} = \frac{I_A}{2} \otimes P \left(\sum_{b=0}^1 \sqrt{p_B(b)} |b\rangle_B \otimes |f_b\rangle_E \right). \quad (9)$$

Above, we define $P(|z\rangle)$ to be $P(|z\rangle) = [z]$. Note we do not make any assumptions on the states $|f_b\rangle$ held by Eve other than they be normalized. We also do not make any assumptions on $p_B(b)$, which is the probability that Bob distills a raw key bit of b , conditioned on Alice initially sending no photons. This distribution may be set by Eve and is part of her attack strategy.

Of course, we may purify Alice's system by adding an extra system R which Eve will not be allowed to access. Thus, the final vacuum state we consider will be:

$$\rho_{ABER}^{(vac)} = P \left(\sum_{a=0}^1 \frac{1}{\sqrt{2}} |a\rangle_A |a\rangle_R \sum_{b=0}^1 \sqrt{p_B(b)} |b\rangle_B \otimes |f_b\rangle_E \right). \quad (10)$$

Now, consider a single photon round. Alice and Bob may symmetrize their bits, causing the joint state shared between Alice and Bob to be Bell diagonal [23, 10]. We may give Eve a purification of this state which can only be to her advantage. Thus, a single photon round is of the form:

$$\rho_{ABE}^{(single)} = P \left(\sum_{x,y \in \{0,1\}} \sqrt{\lambda_x^y} |\phi_x^y\rangle_{AB} |e_x^y\rangle_E \right), \quad (11)$$

where we may assume the $|e_x^y\rangle$ states are orthonormal [23, 10]. Let Q_1 be the raw key error rate in single photon events for Z basis outcomes, and let Q_1^X and Q_1^Y be the error rate in the X and Y basis conditioned on single photon events. One may assume the noise is symmetric in that $Q_1 = Q_1^X = Q_1^Y$, however, this is not required. The following constraints are readily confirmed:

$$\begin{aligned} \lambda_0^1 + \lambda_1^1 &= Q_1^X & \text{(This is the } X \text{ basis error rate in single photon events)} \\ \lambda_1^0 + \lambda_1^1 &= Q_1^Z = Q_1 & \text{(This is the } Z \text{ basis error rate in single photon events)} \\ \lambda_0^1 + \lambda_1^0 &= Q_1^Y & \text{(This is the } Y \text{ basis error rate, if available)} \\ \lambda_0^0 + \lambda_0^1 + \lambda_1^0 + \lambda_1^1 &= 1 & \text{(This is the normalization constraint)} \end{aligned} \quad (12)$$

The above constraints will be important later. Note that we use Q_1 for the Z basis noise (which is also equal to the raw key error rate in single photon rounds, since the Z basis is used for key distillation). We do this, as it will appear in multiple expressions below, and using " Q_1^Z " leads to overly complex notation in the derived expressions. Note also that the third constraint is only available in the three basis (six-state) protocol. Our proof, below, will apply to both the two and three basis version of the decoy state protocol.

Now, consider a block of C raw key rounds, where there are m vacuum events and n single events, with $n + m = C$. We need to compute the von Neumann entropy of such a state after CAD is run and conditioned on CAD accepting the block. Clearly, due to our collective attack assumption, the exact order of these events does not matter – any permutation of the C rounds will lead to the same entropy result. Thus, we may as well analyze a state of the form:

$$\rho_{ABE}^{(m,n)} = \left(\rho_{ABE}^{(vac)} \right)^{\otimes m} \otimes \left(\rho_{ABE}^{(single)} \right)^{\otimes n} \quad (13)$$

Of course, we will analyze the purified version with the additional R ancilla, then later trace out that system which will be equivalent to analyzing the above. Our first step will be to model the CAD process on the above state. To do so, we change basis so that the A and B systems are in the computational basis. Recall from Section 1.1 that $|\phi_x^y\rangle = \frac{1}{\sqrt{2}} \sum_{a=0}^1 (-1)^{a \cdot y} |a, a \oplus x\rangle_{AB}$. By permuting subspaces so that Alice's C bits are in sequential registers, and similarly for Bob's C bits, we may write the purified version of the above density operator $\rho_{ABE}^{(m,n)}$, from Equation 13, in the following manner:

$$\begin{aligned} \rho_{ABER}^{(m,n)} &= \sum_{b \in \{0,1\}^m} \sum_{x,y \in \{0,1\}^n} \sqrt{p_B(b)} \sqrt{\lambda_{x_1}^{y_1} \cdots \lambda_{x_n}^{y_n}} \frac{1}{\sqrt{2^{m+n}}} \\ &\otimes \sum_{\substack{a^{(0)} \in \{0,1\}^m \\ a^{(1)} \in \{0,1\}^n}} (-1)^{a^{(1)} \cdot y} |a^{(0)}, a^{(1)}\rangle_A |b, a^{(1)} \oplus x\rangle_B |f_b, e_x^y\rangle_E |a^{(0)}\rangle_R \end{aligned} \quad (14)$$

Above, $a^{(1)} \cdot y$ is the bit-wise dot product, namely $a_1^{(1)}y_1 + \cdots + a_n^{(1)}y_n$. Note that we distinguish the summation over Alice's C bits by those derived from vacuum events ($a^{(0)}$), and single events ($a^{(1)}$). Above, we write $p_B(b)$, for $b \in \{0,1\}^m$ to mean $p_B(b) = p_B(b_1) \cdots p_B(b_m)$. We also write $|f_b\rangle$ to mean $|f_{b_1}\rangle \otimes \cdots \otimes |f_{b_m}\rangle$ and $|e_x^y\rangle$ to mean $|e_{x_1}^{y_1}\rangle \otimes \cdots \otimes |e_{x_n}^{y_n}\rangle$.

Now, CAD will normally involve all parties measuring the above system in the Z basis, then Alice choosing a random bit k (to be the new candidate key-bit for this block). Alice then broadcasts her measurement result, XOR'd with k . Instead of measuring and performing these operations, we will use delayed measurement techniques, appending the result of the XOR computation into a new ancilla register which will later be measured (and given to Eve). This ancilla will model the classical message sent which is not private, and so Eve will be given this register ultimately. Furthermore, instead of choosing a classical bit k , we will assume Alice prepares the state $|+\rangle_K = \frac{1}{\sqrt{2}}(|0\rangle + |1\rangle)$, then later measures this in the Z basis, causing a collapse to 0 or 1 randomly. It is not difficult to see that this will result in a mathematically equivalent state, however it is easier to analyze this “purified” version of the protocol.

First, Alice creates an ancilla K in the equal superposition state $|+\rangle_K$. She will then create a new C -qubit ancilla register M (for the classical “Message” she sends to Bob), initially cleared to $|0 \cdots 0\rangle_M$. Finally, she will apply a total of C , DCNOT operations, defined in Section 1.1, which will model the CAD XOR computation. The j 'th DCNOT will set the first control to the K ancilla, and the second control on Alice's j 'th qubit in her A register; the target will be set to the j 'th qubit in the M ancilla. In particular, for any $k, a^{(0)}, a^{(1)}$, it will hold that:

$$DCNOT^{\otimes C} |k\rangle_K |a^{(0)}, a^{(1)}\rangle_A |0 \cdots 0\rangle_M = |k\rangle_K |a^{(0)}, a^{(1)}\rangle_A |a^{(0)} \oplus k^m, a^{(1)} \oplus k^n\rangle, \quad (15)$$

where, above, by k^m we mean $k \cdots k$, repeated m times (similarly for k^n). Due to linearity of the above operation, Equation 14, the initial C block state, evolves to the following:

$$\begin{aligned} &\frac{1}{\sqrt{2}} \sum_{k=0}^1 |k\rangle_K \sum_{b \in \{0,1\}^m} \sum_{x,y \in \{0,1\}^n} \sqrt{p_B(b)} \sqrt{\lambda_{x_1}^{y_1} \cdots \lambda_{x_n}^{y_n}} \frac{1}{\sqrt{2^{m+n}}} \\ &\otimes \sum_{\substack{a^{(0)} \in \{0,1\}^m \\ a^{(1)} \in \{0,1\}^n}} (-1)^{a^{(1)} \cdot y} |a^{(0)}, a^{(1)}\rangle_A |b, a^{(1)} \oplus x\rangle_B |a^{(0)} \oplus k^m, a^{(1)} \oplus k^n\rangle_M |f_b, e_x^y\rangle_E |a^{(0)}\rangle_R. \end{aligned} \quad (16)$$

By permuting subspaces so that the message ancilla M appears first and Eve's systems last, and also by recalling that $m + n = C$, we may write the above state as:

$$\frac{1}{\sqrt{2^C}} \sum_{\substack{p^{(0)} \in \{0,1\}^m \\ p^{(1)} \in \{0,1\}^n}} |p^{(0)}, p^{(1)}\rangle_M \sum_{b \in \{0,1\}^m} \sum_{x,y \in \{0,1\}^n} \sqrt{p_B(b)} \sqrt{\lambda_{x_1}^{y_1} \cdots \lambda_{x_n}^{y_n}} \otimes \quad (17)$$

$$\begin{aligned} & \left((-1)^{y \cdot p^{(1)}} \frac{1}{\sqrt{2}} |0\rangle_K |p^{(0)}, p^{(1)}\rangle_A |b, p^{(1)} \oplus x\rangle_B |p^{(0)}\rangle_R \right. \\ & \left. + (-1)^{y \cdot \bar{p}^{(1)}} \frac{1}{\sqrt{2}} |1\rangle_K |\bar{p}^{(0)}, \bar{p}^{(1)}\rangle_A |b, \bar{p}^{(1)} \oplus x\rangle_B |\bar{p}^{(0)}\rangle_R \right) \\ & \otimes |f_b, e_x^y\rangle_E \end{aligned} \quad (18)$$

We use $p^{(0)}$ and $p^{(1)}$ to represent the “Public” message sent by Alice in the M register, consistent with our notation in Section 1.1. Recall that $\bar{x} = 1 - x = 1 \oplus x$ for a single bit x , while for an n -bit string $x = x_1 \cdots x_n$, we write \bar{x} to mean $\bar{x}_1 \cdots \bar{x}_n = 1 \cdots 1 \oplus x_1 \cdots x_n$. Note that the phase exponent of the $K = 1$ term is $y \cdot \bar{p}^{(1)} = y \cdot (p^{(1)} \oplus 1 \cdots 1)$. It is easy to verify that $(-1)^{p^{(1)} \cdot y} (-1)^{\bar{p}^{(1)} \cdot y} = (-1)^{y_1 + \cdots + y_n}$. Thus, we can write the above as:

$$\begin{aligned} & \frac{1}{\sqrt{2^C}} \sum_{\substack{p^{(0)} \in \{0,1\}^m \\ p^{(1)} \in \{0,1\}^n}} |p^{(0)}, p^{(1)}\rangle_M \sum_{b \in \{0,1\}^m} \sum_{x,y \in \{0,1\}^n} (-1)^{y \cdot p^{(1)}} \sqrt{p_B(b)} \sqrt{\lambda_{x_1}^{y_1} \cdots \lambda_{x_n}^{y_n}} \otimes \\ & \left(\frac{1}{\sqrt{2}} |0\rangle_K |p^{(0)}, p^{(1)}\rangle_A |b, p^{(1)} \oplus x\rangle_B |p^{(0)}\rangle_R + (-1)^{y_1 + \cdots + y_n} \frac{1}{\sqrt{2}} |1\rangle_K |\bar{p}^{(0)}, \bar{p}^{(1)}\rangle_A |b, \bar{p}^{(1)} \oplus x\rangle_B |\bar{p}^{(0)}\rangle_R \right) \\ & \otimes |f_b, e_x^y\rangle \end{aligned} \quad (19)$$

The above represents the joint state modeling the system after Alice's public announcement, in the purified version of the protocol. At this point, let's measure the M register and condition on a particular message $p^{(0)}$ and $p^{(1)}$; this simulates the case where Alice and Bob run the CAD process and Alice sends this particular classical message. First, we compute $Pr(M = p^{(0)}p^{(1)})$, the probability that this particular message is sent. Due to the orthogonality assumption on Eve's vectors $|e_x^y\rangle$ (note we do not assume anything about $|f_b\rangle$ other than they are normalized), this is readily computed from Equation 19 to be:

$$Pr(M = p^{(0)}p^{(1)}) = \frac{1}{2^C} \sum_{b \in \{0,1\}^m} \sum_{x,y \in \{0,1\}^n} p_B(b) \lambda_{x_1}^{y_1} \cdots \lambda_{x_n}^{y_n} = \frac{1}{2^C}. \quad (20)$$

Thus, all possible messages from Alice can occur, uniformly at random. We will now condition on a particular message, and analyze the entropy in the post-measured state; the total von Neumann entropy will be the average entropy across all messages (see Section 1.1). Conditioning on $M = p^{(0)}p^{(1)}$, and using Equation 20, the post measured state collapses to:

$$\begin{aligned} & \sum_{b \in \{0,1\}^m} \sum_{x,y \in \{0,1\}^n} (-1)^{y \cdot p^{(1)}} \sqrt{p_B(b)} \sqrt{\lambda_{x_1}^{y_1} \cdots \lambda_{x_n}^{y_n}} \otimes \\ & \left(\frac{1}{\sqrt{2}} |0\rangle_K |p^{(0)}, p^{(1)}\rangle_A |b, p^{(1)} \oplus x\rangle_B |p^{(0)}\rangle_R + (-1)^{y_1 + \cdots + y_n} \frac{1}{\sqrt{2}} |1\rangle_K |\bar{p}^{(0)}, \bar{p}^{(1)}\rangle_A |b, \bar{p}^{(1)} \oplus x\rangle_B |\bar{p}^{(0)}\rangle_R \right) \\ & \otimes |f_b, e_x^y\rangle \end{aligned} \quad (21)$$

Normally parties will measure the A and B registers (the R register would be discarded) and Bob will determine whether this block should be accepted or rejected. However, let's consider the next stage of the protocol: Bob's computation and decision to accept or reject this block. Now, Bob will only accept this particular round if his B register (after making a Z basis measurement), XOR'd with the M register results in the all zero string or the all one string. It is not difficult to see that he will accept the above state only if the following two conditions are *both* satisfied:

1. $b \oplus p^{(0)} = 0 \cdots 0$ or $1 \cdots 1$
2. $(p^{(1)} \oplus x) \oplus p^{(1)} = 0 \cdots 0$ or $1 \cdots 1$ OR $(\bar{p}^{(1)} \oplus x) \oplus p^{(1)} = 0 \cdots 0$ or $1 \cdots 1$.

The first constraint is satisfied if $b = p^{(0)}$ or $b = \bar{p}^{(0)}$ while the second constraint is satisfied only if $x = 0 \cdots 0$ or $x = 1 \cdots 1$.

While normally parties would measure their systems and perform the necessary check as dictated by CAD, it is equivalent to perform a two-outcome measurement, projecting the state to an accepting one (i.e., one where the above constraints are satisfied), or a rejected state (one where the above constraints are not satisfied). Parties may then later measure as normal; ultimately the distribution and resulting outcomes will be identical. However, as with our previous delayed measurements, it is easier to perform this projection and analyze the accepted, pure, state. Conditioning on an accepting state (any rejected state will be discarded and so we do not analyze it), the post measured state collapses to:

$$\begin{aligned} & \frac{1}{\sqrt{p_a}} \sum_{b=0}^1 \sqrt{p_B(p^{(0)} \oplus b^m)} \sum_{x=0}^1 \sum_{y \in \{0,1\}^n} (-1)^{y \cdot p^{(1)}} \sqrt{\lambda_x^{y_1} \cdots \lambda_x^{y_n}} \otimes \\ & \left(\frac{1}{\sqrt{2}} |0\rangle_K |p^{(0)}, p^{(1)}\rangle_A |p^{(0)} \oplus b^m, p^{(1)} \oplus x^n\rangle_B |p^{(0)}\rangle_R \right. \\ & \left. + (-1)^{y_1 + \cdots + y_n} \frac{1}{\sqrt{2}} |1\rangle_K |\bar{p}^{(0)}, \bar{p}^{(1)}\rangle_A |p^{(0)} \oplus b^m, \bar{p}^{(1)} \oplus x^n\rangle_B |\bar{p}^{(0)}\rangle_R \right) \\ & \otimes |f_{p^{(0)} \oplus b^m}, e_{x^n}^y\rangle \end{aligned} \quad (22)$$

Note that, in the above, we index now over single bit $b = 0, 1$ and a single bit $x = 0, 1$ due to the constraints required for Bob to accept. Above, p_a is a normalization term which, in this case, is the probability of Bob accepting this block, conditioned on this particular message choice. We readily compute this to be:

$$p_a = \Pr(\text{acc} | M = p^{(0)}p^{(1)}) = \sum_{b=0}^1 p_B(p^{(0)} \oplus b^m) \sum_{x=0}^1 \sum_{y \in \{0,1\}^n} \lambda_x^{y_1} \cdots \lambda_x^{y_n} \quad (23)$$

Recall from Equation 12, that $Q_1 = \lambda_1^0 + \lambda_1^1$ and, so, $1 - Q_1 = \lambda_0^0 + \lambda_0^1$. Thus:

$$\begin{aligned} Q_1^n &= \sum_{y \in \{0,1\}^n} \lambda_1^{y_1} \cdots \lambda_1^{y_n} \\ (1 - Q_1)^n &= \sum_{y \in \{0,1\}^n} \lambda_0^{y_1} \cdots \lambda_0^{y_n} \end{aligned} \quad (24)$$

Thus, Equation 23 becomes:

$$p_a = \sum_{b=0}^1 p_B(p^{(0)} \oplus b^m)(Q_1^n + (1 - Q_1)^n). \quad (25)$$

Note that the distribution Eve chooses for Bob, p_B , can influence the above. However, Eve cannot set the distribution in such a way that Bob *always* rejects; indeed, there must be at least one message $p^{(0)}p^{(1)}$ where $p_a > 0$ (otherwise, $p_B(b) = 0$ for all b which is impossible). Thus, we assume, here, that the message we condition on is one that could show up in the protocol (i.e., where $p_a > 0$).

Note that, while Eve can influence the probability that Bob accepts this block conditioned on a particular message, on average over all messages, Eve's attack will not influence the total probability of accepting a block. Indeed, let Q_0 be the probability of error in the vacuum round case; clearly this is $Q_0 = 1/2$ since there is no correlation in Alice and Bob's register. Then, the probability of accepting, over *all* possible messages is:

$$\begin{aligned} Pr(acc) &= \sum_{\substack{p^{(0)} \in \{0,1\}^m \\ p^{(1)} \in \{0,1\}^n}} Pr(M = p^{(0)}p^{(1)}) Pr(acc|M = p^{(0)}p^{(1)}) \\ &= \frac{1}{2^C} \sum_{\substack{p^{(0)} \in \{0,1\}^m \\ p^{(1)} \in \{0,1\}^n}} \sum_{b=0}^1 p_B(p^{(0)} \oplus b^m)(Q_1^n + (1 - Q_1)^n) \\ &= \frac{1}{2^{m+n}} \times 2^n \left(\sum_{p^{(0)} \in \{0,1\}^m} p_B(p^{(0)}) + \sum_{p^{(0)} \in \{0,1\}^m} p_B(\bar{p}^{(0)}) \right) \times (Q_1^n + (1 - Q_1)^n) \\ &= \frac{2}{2^m} (Q_1^n + (1 - Q_1)^n) = (Q_0^m + (1 - Q_0)^m) (Q_1^n + (1 - Q_1)^n) \end{aligned} \quad (26)$$

Above, we used the fact that $\sum_{p^{(0)}} p_B(p^{(0)}) = \sum_{p^{(0)}} p_B(\bar{p}^{(0)}) = 1$, and also that $Q_0 = 1/2$. Thus, while Eve can influence the conditional probability of accepting this block, the total probability is immune to Eve's probability distribution p_B in vacuum events, which makes sense. The above identity will be important later; however, for now, we return to the conditional case of analyzing the entropy in a *particular* message $M = p^{(0)}p^{(1)}$.

We are now in a position to compute the conditional entropy between the K register and Eve's ancilla. This is derived in the following lemma:

Lemma 1. Consider the state described in Equation 22, where p_a (defined in Equation 25) is non-zero. Assume a measurement is made of the K register, while the A , B , and R registers are discarded (equivalently, they are measured, then discarded). Then, it holds that the conditional entropy $H(K|E, M = p^{(0)}p^{(1)})$ in the resulting state is lower-bounded by:

$$\begin{aligned} H(K|E, M = p^{(0)}p^{(1)}) &\geq f(\lambda_0^1, \lambda_1^0, \lambda_1^1) \\ &:= \frac{(1 - Q_1)^n}{Q_1^n + (1 - Q_1)^n} \left(1 - h \left[\frac{1}{2} \left(1 + \frac{|(1 - Q_1)^n - 2\Lambda_0|}{(1 - Q_1)^n} \right) \right] \right) \\ &\quad + \frac{Q_1^n}{Q_1^n + (1 - Q_1)^n} \left(1 - h \left[\frac{1}{2} \left(1 + \frac{|Q_1^n - 2\Lambda_1|}{Q_1^n} \right) \right] \right), \end{aligned} \quad (27)$$

where $Q_1 = \lambda_1^0 + \lambda_1^1$, and:

$$\Lambda_x = \sum_{j=0}^{\lfloor \frac{n}{2} \rfloor} \binom{n}{2j} (\lambda_x^1)^{2j} (\lambda_x^0)^{n-2j}. \quad (28)$$

In the above, we have $\lambda_0^0 = 1 - \lambda_1^0 - \lambda_0^1 - \lambda_1^1$, and recall that n is the number of single photon rounds in the given block of C raw key bits.

Proof. We start with the case where $m > 0$ (i.e., there is at least one vacuum case). The case where $m = 0$ will follow. Measuring the K register of the state after running CAD, namely Equation 22, while discarding the A , B , and R registers, yields the following mixed state:

$$\begin{aligned} & \frac{1}{2p_a} [0]_K \otimes \left(\sum_{b=0}^1 \sum_{x=0}^1 P \left(\sqrt{p_B(p^{(0)} \oplus b^m)} \sum_{y \in \{0,1\}^n} (-1)^{p^{(1)} \cdot y} \sqrt{\lambda_x^{y_1} \cdots \lambda_x^{y_n}} |f_b e_{x^n}^y\rangle \right) \right) \\ & + \frac{1}{2p_a} [1]_K \otimes \left(\sum_{b=0}^1 \sum_{x=0}^1 P \left(\sqrt{p_B(p^{(0)} \oplus b^m)} \sum_{y \in \{0,1\}^n} (-1)^{p^{(1)} \cdot y} (-1)^{y_1 + \cdots + y_n} \sqrt{\lambda_x^{y_1} \cdots \lambda_x^{y_n}} |f_b, e_{x^n}^y\rangle \right) \right). \end{aligned} \quad (29)$$

Above, recall that $P(|z\rangle) = |z\rangle\langle z|$. Note that, by $|f_b\rangle$ above, we actually mean $|f_{p^{(0)} \oplus b^m}\rangle$, however to avoid complicated notation, we will simply write $|f_b\rangle$ above; since $p^{(0)}$ is fixed, it does not help to write the entire subscript out, while it would hinder readability. We will be using this change of notation throughout the rest of the proof.

Consider the following operator $V_{p^{(1)}}$ which maps $|f_b, e_{x^n}^y\rangle$ to $(-1)^{y \cdot p^{(1)}} |f_b, e_{x^n}^y\rangle$. Since $|e_x^y\rangle$ are orthogonal (a condition of the given input state as discussed in the narrative above), and since $p^{(0)}, p^{(1)}$ are fixed and public knowledge, it is easy to see that this map is unitary. Since unitary changes of basis do not affect entropy, we may apply this map to the E system, resulting in the following density operator:

$$\begin{aligned} \rho_{KE} = & \frac{1}{2p_a} [0]_K \otimes \left(\sum_{b=0}^1 \sum_{x=0}^1 P \left(\sqrt{p_B(p^{(0)} \oplus b^m)} \sum_{y \in \{0,1\}^n} \sqrt{\lambda_x^{y_1} \cdots \lambda_x^{y_n}} |f_b e_{x^n}^y\rangle \right) \right) \\ & + \frac{1}{2p_a} [1]_K \otimes \left(\sum_{b=0}^1 \sum_{x=0}^1 P \left(\sqrt{p_B(p^{(0)} \oplus b^m)} \sum_{y \in \{0,1\}^n} (-1)^{y_1 + \cdots + y_n} \sqrt{\lambda_x^{y_1} \cdots \lambda_x^{y_n}} |f_b, e_{x^n}^y\rangle \right) \right). \end{aligned} \quad (30)$$

The conditional entropy in the state ρ_{KE} , above, will be equal to that of Equation 29, where $V_{p^{(1)}}$ was not applied.

Now, for $b, k, x \in \{0, 1\}$, define the following vectors in Eve's ancilla:

$$|E_{b,x}^k\rangle = \sqrt{p_B(p^{(0)} \oplus b^m)} \sum_{y \in \{0,1\}^n} (-1)^{k \cdot (y_1 + \cdots + y_n)} \sqrt{\lambda_x^{y_1} \cdots \lambda_x^{y_n}} |f_b, e_{x^n}^y\rangle. \quad (31)$$

With this, we may simplify Equation 30 to:

$$\rho_{KE} = \frac{1}{2p_a} [0]_K \otimes \left(\sum_{b,x \in \{0,1\}} [E_{b,x}^0] \right) + \frac{1}{2p_a} [1]_K \otimes \left(\sum_{b,x \in \{0,1\}} [E_{b,x}^1] \right) \quad (32)$$

Using Theorem 1, we can bound the entropy in the above state by the following expression:

$$H(K|E)_\rho \geq \sum_{b,x} \frac{\langle E_{b,x}^0 | E_{b,x}^0 \rangle + \langle E_{b,x}^1 | E_{b,x}^1 \rangle}{2p_a} \left(h \left[\frac{\langle E_{b,x}^0 | E_{b,x}^0 \rangle}{\langle E_{b,x}^0 | E_{b,x}^0 \rangle + \langle E_{b,x}^1 | E_{b,x}^1 \rangle} \right] - h[\nu_{x,y}] \right), \quad (33)$$

where:

$$\nu_{b,x} = \frac{1}{2} \left(1 + \frac{\sqrt{\left(\langle E_{b,x}^0 | E_{b,x}^0 \rangle - \langle E_{b,x}^1 | E_{b,x}^1 \rangle \right)^2 + 4Re^2 \langle E_{b,x}^0 | E_{b,x}^1 \rangle}}{\langle E_{b,x}^0 | E_{b,x}^0 \rangle + \langle E_{b,x}^1 | E_{b,x}^1 \rangle} \right). \quad (34)$$

Note, we are not bothering to write the conditional $M = p^{(0)}p^{(1)}$ in the entropy function (Equation 33), in order to avoid unnecessary notation; however, of course, we are still conditioning on this particular message.

Now, the inner-product $\langle E_{b,x}^k | E_{b,x}^k \rangle$ is found to be:

$$\langle E_{b,x}^k | E_{b,x}^k \rangle = p_B(p^{(0)} \oplus b^m) \sum_{y \in \{0,1\}^n} \lambda_x^{y_1} \dots \lambda_x^{y_n} = p_B(p^{(0)} \oplus b^m) P_x \quad (35)$$

where, by Equation 24:

$$P_x = \sum_{y \in \{0,1\}^n} \lambda_x^{y_1} \dots \lambda_x^{y_n} = \begin{cases} (1 - Q_1)^n & \text{if } x = 0 \\ Q_1^n & \text{if } x = 1 \end{cases} \quad (36)$$

Note that $\langle E_{b,x}^0 | E_{b,x}^0 \rangle = \langle E_{b,x}^1 | E_{b,x}^1 \rangle$ for all b and x . For the inner products $\langle E_{b,x}^0 | E_{b,x}^1 \rangle$, we find:

$$\langle E_{b,x}^0 | E_{b,x}^1 \rangle = p_B(p^{(0)} \oplus b^m) \sum_{y \in \{0,1\}^n} (-1)^{y_1 + \dots + y_n} \lambda_x^{y_1} \dots \lambda_x^{y_n} \quad (37)$$

Substituting Equation 35 and 37 into Equation 34, we can simplify to:

$$\begin{aligned} \nu_{b,x} &= \frac{1}{2} \left(1 + \frac{\left| p_B(p^{(0)} \oplus b^m) \sum_{y \in \{0,1\}^n} (-1)^{y_1 + \dots + y_n} \lambda_x^{y_1} \dots \lambda_x^{y_n} \right|}{p_B(p^{(0)} \oplus b^m) P_x} \right) \\ &= \frac{1}{2} \left(1 + \frac{\left| \sum_{y \in \{0,1\}^n} (-1)^{y_1 + \dots + y_n} \lambda_x^{y_1} \dots \lambda_x^{y_n} \right|}{P_x} \right) \\ &= \nu_x, \end{aligned} \quad (38)$$

Since there is no dependence on b , we may denote $\nu_{b,x}$ by ν_x as done above. Thus, Equation 33 simplifies to:

$$\begin{aligned} H(K|E) &\geq \sum_{x=0}^1 \left(\sum_{b=0}^1 \frac{\langle E_{b,x}^0 | E_{b,x}^0 \rangle + \langle E_{b,x}^1 | E_{b,x}^1 \rangle}{2p_a} \right) (1 - h[\nu_x]) \\ &= \sum_x \frac{(p_B(p^{(0)} \oplus 0 \dots 0) + p_B(p^{(0)} \oplus 1 \dots 1)) P_x}{p_a} (1 - h[\nu_x]) \\ &= \sum_x \frac{P_x}{P_0 + P_1} (1 - h[\nu_x]) \end{aligned} \quad (39)$$

For the last equality, above, note that we can write p_a (from Equation 23) as $p_a = p_B(p^{(0)})(P_0 + P_1) + p_B(p^{(0)} \oplus 1 \cdots 1)(P_0 + P_1)$.

Now, returning to Equation 37, let $\text{Even}[n]$ be the set of all n bit strings $y \in \{0, 1\}^n$ such that the sum $y_1 + \cdots + y_n$ is even, while $\text{Odd}[n]$ is the set of all n bit strings where $y_1 + \cdots + y_n$ is odd. Then, noting that $P_x = \sum_{y \in \text{Even}[n]} \lambda_x^{y_1} \cdots \lambda_x^{y_n} + \sum_{y \in \text{Odd}[n]} \lambda_x^{y_1} \cdots \lambda_x^{y_n}$, we can solve:

$$\begin{aligned} |\langle E_{x,b}^0 | E_{x,b}^1 \rangle| &= p_B(p^{(0)} \oplus b^m) \left| \sum_{y \in \text{Even}[n]} \lambda_x^{y_1} \cdots \lambda_x^{y_n} - \sum_{y \in \text{Odd}[n]} \lambda_x^{y_1} \cdots \lambda_x^{y_n} \right| \\ &= p_B(p^{(0)} \oplus b^m) \left| P_x - 2 \sum_{y \in \text{Even}[n]} \lambda_x^{y_1} \cdots \lambda_x^{y_n} \right|. \end{aligned} \quad (40)$$

Let $\Lambda_x = \sum_{y \in \text{Even}[n]} \lambda_x^{y_1} \cdots \lambda_x^{y_n}$ which we can compute as:

$$\Lambda_x = \sum_{y \in \text{Even}[n]} \lambda_x^{y_1} \cdots \lambda_x^{y_n} = \sum_{j=0}^{\lfloor \frac{n}{2} \rfloor} \binom{n}{2j} (\lambda_x^1)^{2j} (\lambda_x^0)^{n-2j}. \quad (41)$$

as defined in the lemma statement. Combining all of this with Equations 38 and 39, yields the lemma statement.

Of course, the above assumed $m > 0$. If $m = 0$ (and, thus, $n = C$ so there are only single-photon events in this block), it is straight-forward to apply the above analysis, ignoring the vacuum system (i.e., removing the sum over b and the $|f_b\rangle$ systems in the analysis above). The result will be the same as above, which has no dependence on m or b , thus completing the proof. \square

Of course, the above was only for a specific message $M = p^{(0)}p^{(1)}$ such that the probability of Bob accepting is non-zero. However, we note that our bound does not depend on the message itself. We can thus prove the following:

Theorem 2. Let $\rho_{ABE}^{(m,n)}$ be the state describing C rounds of the BB84 protocol, before CAD is run, where:

$$\rho_{ABE}^{(m,n)} \cong \left(\rho_{ABE}^{(vac)} \right)^{\otimes m} \otimes \left(\rho_{ABE}^{(single)} \right)^{\otimes n} \quad (42)$$

where by “ \cong ”, we mean equal, up to a permutation of the C rounds. Let Q_1^Z , Q_1^X , and Q_1^Y denote the Z , X , and Y basis errors of a single round, in the single photon case (i.e., for a state of the form $\rho_{ABE}^{(single)}$). Note that Q_1^Y may not be available if using the four state BB84.

Now, assume the CAD process is run on the above state resulting in mixed state $\rho_{KEM}^{(m,n)}$ (where we discard the A and B systems). Then it holds that in the four state (BB84) protocol:

$$H(K|EM) \geq \min_{\lambda_1^1} f(Q_1^X - \lambda_1^1, Q_1^Z - \lambda_1^1, \lambda_1^1) \quad (43)$$

where the minimum, above, is over $|\lambda_1^1| \leq \min(Q_1^X, Q_1^Z)$. For the six-state version, we have:

$$H(K|E) \geq f\left(\frac{1}{2}(Q_1^X + Q_1^Y - Q_1^Z), \frac{1}{2}(Q_1^Y + Q_1^Z - Q_1^X), \frac{1}{2}(Q_1^X + Q_1^Z - Q_1^Y)\right) \quad (44)$$

Above, $f(a, b, c)$ is the function defined in Lemma 1.

Proof. This is now straight-forward to show given the above results. Indeed, after running CAD on the above input state, and conditioned on Bob accepting, the resulting system becomes a mixture over all possible messages $p^{(0)}p^{(1)}$ that could be sent by Alice and where Bob has a non-zero probability of accepting. As discussed above, at least one message has a non-zero probability of accepting. Tracing out Alice and Bob on such a state, the von Neumann entropy will simply be the average entropy across all messages. Since the bound derived in Lemma 1 does not depend on the message itself, the result follows from basic properties of von Neumann entropy.

Of course, Lemma 1 assumed λ_x^y were known exactly; thus we must minimize over all possibilities subject to the constraints in Equation 12. In the four state version, only one variable is free, while in the six-state version, one may solve for each λ_x^y directly, yielding the theorem statement. \square

3.2 Asymptotic Key Rate Bound

The above analyzed a particular block of C rounds, with a fixed number of photons for each round, namely m vacuum events and n single photon events. We now analyze the entire protocol, using the above results, to derive a general key-rate bound for the decoy state protocol in the asymptotic scenario. As discussed, we will first assume collective attacks, whereby Eve attacks each round independently and identically which will allow us to immediately use our analysis in the previous section. Later we will promote this to security against general attacks using standard techniques.

Let ρ_{ABE} be the state describing one round of the quantum communication stage of the protocol (before CAD is run), conditioning on Alice and Bob distilling a raw key bit (that is, Bob did not observe a vacuum). In this case, the A and B registers store Alice and Bob's raw key bit for this round, again before CAD is run. It is not difficult to see that this state is of the form:

$$\rho_{ABE} = \sum_{n \geq 0} G_n \rho_{ABE}^{(n)}, \quad (45)$$

where $G_n = p(n|acc)$ is the probability that Alice initially sent n photons, conditioned on both Alice and Bob accepting this round (namely, conditioned on Bob making a non-vacuum observation). Of course, $\rho_{ABE}^{(n)}$ is the conditional state where Alice sent n photons, and Bob distilled a key-bit (i.e., his detectors did not observe a vacuum).

Now, CAD will be run on a block of C rounds. The state, before CAD is run, is of the form:

$$\rho_{ABE}^{\otimes C} = \sum_{n_1, \dots, n_C \geq 0} G_{n_1} \cdots G_{n_C} \rho_{ABE}^{(n_1)} \otimes \cdots \otimes \rho_{ABE}^{(n_C)}. \quad (46)$$

Let $\mathcal{C}_{n_1 \dots n_C}$ be the probability that Alice and Bob's CAD process accepts a block of C bits, conditioned on Alice initially sending n_1 photons in the first round, n_2 photons in the second, and so on (and, of course, conditioned on Alice and Bob distilling a raw key - i.e., Bob not observing a vacuum in any of the C rounds). This probability is based on the error rate in an n_1, \dots, n_C photon state. Let Q_n be the probability that Alice and Bob have different raw key bits (namely, different Z basis measurements), conditioned on Alice initially sending n photons and Bob not observing a vacuum. That is, Q_n is the Z error rate in $\rho_{ABE}^{(n)}$. Then it is easy to see that (also see Equation 26 and the surrounding discussion):

$$\mathcal{C}_{n_1 \dots n_C} = Q_{n_1} Q_{n_2} \cdots Q_{n_C} + (1 - Q_{n_1})(1 - Q_{n_2}) \cdots (1 - Q_{n_C}). \quad (47)$$

Of course, Q_n , along with G_n are not directly observable; however, the decoy state method can be used to provide good bounds for these, based on the average observed error and gain, as we will discuss later in detail, in Section 3.3.

Using the above notation, this C -bit block (Equation 46), after running CAD, is found to be:

$$\begin{aligned}\rho_{ABE}^{\otimes C} &= \sum_{n_1, \dots, n_C \geq 0} G_{n_1} \cdots G_{n_C} \rho_{ABE}^{(n_1)} \otimes \cdots \otimes \rho_{ABE}^{(n_C)} \\ &\mapsto \sum_{n_1, \dots, n_C \geq 0} G_{n_1} \cdots G_{n_C} \left(\mathcal{C}_{n_1 \dots n_C} \rho_{KEM}^{(n_1 \dots n_C)} + (1 - \mathcal{C}_{n_1 \dots n_C}) \sigma_{KEM}^{(n_1 \dots n_C)} \right)\end{aligned}\quad (48)$$

where $\rho_{KEM}^{(n_1 \dots n_C)}$ is the conditional state, after CAD, where Alice initially sent n_1, n_2, \dots, n_C photons, and conditioned on CAD accepting the block; $\sigma_{KEM}^{(n_1 \dots n_C)}$ is the same, but conditioned on parties rejecting the CAD block. Conditioning on accepting this block, the above state becomes:

$$\rho_{KEM} = \frac{1}{\mathcal{C}_{total}} \sum_{n_1, \dots, n_C \geq 0} G_{n_1} \cdots G_{n_C} \mathcal{C}_{n_1 \dots n_C} \rho_{KEM}^{(n_1 \dots n_C)}, \quad (49)$$

where \mathcal{C}_{total} is a normalization term, namely the total probability of Alice and Bob accepting this block. From Equation 48, and using Equation 47, this is readily found to be:

$$\begin{aligned}\mathcal{C}_{total} &= \sum_{n_1, \dots, n_C \geq 0} G_1 \cdots G_{n_C} \mathcal{C}_{n_1 \dots n_C} \\ &= \sum_{n_1, \dots, n_C \geq 0} G_1 \cdots G_{n_C} Q_{n_1} \cdots Q_{n_C} + \sum_{n_1, \dots, n_C \geq 0} G_1 \cdots G_{n_C} (1 - Q_{n_1}) \cdots (1 - Q_{n_C})\end{aligned}\quad (50)$$

Consider the average *observed* error in any one particular round using the signal state power level μ . We denote this observed error by Q_μ , and it is clearly found to be:

$$Pr(A \neq B) = Q_\mu = \sum_{n \geq 0} G_n Q_n \quad (51)$$

$$Pr(A = B) = \sum_{n \geq 0} G_n (1 - Q_n) = 1 - Q_\mu. \quad (52)$$

Then, Q_μ^C can be written as $Q_\mu^C = \sum_{n_1, \dots, n_C \geq 0} G_{n_1} \cdots G_{n_C} Q_{n_1} \cdots Q_{n_C}$. A similar expression can be found for $(1 - Q_\mu)^C$. Thus, Equation 50 becomes:

$$\mathcal{C}_{total} = Q_\mu^C + (1 - Q_\mu)^C, \quad (53)$$

as expected, since CAD accepts a block only if all C rounds are non-error events, or all C rounds are error events.

Now, to compute the key-rate, we need to determine the entropy in the K register of Equation 49. To do so, we will of course utilize our Theorem 2. First, note that Alice and Bob may perform a symmetrization step, before CAD runs, to ensure their states are Bell diagonal [23, 10]; giving Eve the purification can only help her. Thus the requirement on the orthogonality of the ancilla vectors of Theorem 2 holds. It is also not difficult to see that this requirement also holds under symmetric

noise (i.e., a depolarization channel) without this symmetrization step. By basic properties of von Neumann entropy (see Section 1.1), we have:

$$H(K|EM) \geq \frac{1}{C_{total}} \sum_{n_1, \dots, n_C} G_{n_1} \dots G_{n_C} \mathcal{C}_{n_1 \dots n_C} H(K|EM)_{\rho^{(n_1, \dots, n_C)}} \quad (54)$$

Since there is a clear attack for Eve to follow which gains her full information whenever $n_i \geq 2$ for any particular round (see Section 2), we must assume $H(K|EM)_{\rho^{(n_1, \dots, n_C)}} = 0$ whenever $n_i \geq 2$ for some i . Now, consider a particular $\rho_{KEM}^{(n_1, \dots, n_C)}$ where there are m rounds where $n_i = 0$ and n rounds where $n_i = 1$, with $m + n = C$. Clearly due to our i.i.d. assumptions the exact ordering of these rounds is irrelevant (see also Section 3.1). Thus, we may bound Equation 54 using our Theorem 2 as follows:

$$H(K|EM) \geq \frac{1}{C_{total}} \sum_{n=0}^C \binom{C}{n} G_1^n G_0^{C-n} \frac{1}{2^{C-n}} (Q_1^n + (1 - Q_1)^n) h_n, \quad (55)$$

where h_n is the result of the minimization in Theorem 2 for a state with n single photon rounds and $C - n$ vacuum rounds. This, of course, depends also on Q_1^X , Q_1^Z , and potentially Q_1^Y if available. Note that, above, we used the fact that $\mathcal{C}_{n_1 \dots n_C}$, appearing inside the above summation (where n is the number of single photon rounds, and $C - n$ is the number of vacuum rounds), can be written as $\frac{1}{2^{C-n}} (Q_1^n + (1 - Q_1)^n)$, which is readily confirmed from Equation 47, recalling that $Q_0 = 1/2$.

Equation 55 is our final conditional entropy bound, for the state consisting of a CAD block of size C , conditioned on Alice and Bob distilling a key-bit. Of course, we are really interested in the *effective* key rate, namely the relative size of the final secret key, to the total number of rounds sent, including those which were discarded in the quantum communication stage - i.e., those rounds where Bob saw a vacuum. Let N be the total number of rounds in the decoy state protocol. Since we are in the asymptotic setting, we may set the probability of basis mismatch to be arbitrarily close to zero and the probability of using the signal power level to be arbitrarily close to one; thus we do not need to consider loss due to basis mismatch in the asymptotic key-rate.

Let μ be the power level used for signal states. Then, let G_μ be the probability of Alice and Bob distilling a raw key bit in the quantum communication stage, when power level μ is used. Thus, after communicating N times in the quantum communication stage of the protocol, it is expected that $G_\mu N$ raw key bits will be distilled (before CAD). From these, CAD is run which will accept a block of C bits with probability \mathcal{C}_{total} . Furthermore, the total number of raw key bits will also be divided by C , since an entire block can only lead to one raw key bit. In summary, out of the N rounds, one will expect a final raw key size (after CAD) of $G_\mu \mathcal{C}_{total} N / C$.

Using Equations 55 and 6, along with our above analysis, specifically Equation 55, we may determine the final secret key rate to be:

$$\begin{aligned} r_\infty &\geq \frac{G_\mu \mathcal{C}_{total}}{C} (H(K|EM) - H(K|B)) \\ &\geq \frac{G_\mu}{C} \left(\sum_{n=0}^C \binom{C}{n} G_1^n G_0^{C-n} \frac{1}{2^{C-n}} (Q_1^n + (1 - Q_1)^n) h_n - H(K|B) \right) \end{aligned}$$

where $H(K|B)$ is the conditional entropy between Alice's new key register K (the raw key bit after CAD), and Bob's new raw key bit register after he runs CAD. This is clearly found to be:

$$H(K|B) = h \left(\frac{Q_\mu^C}{Q_\mu^C + (1 - Q_\mu)^C} \right). \quad (56)$$

Thus, we determine the final effective asymptotic key-rate expression to be:

$$r_\infty \geq \frac{G_\mu}{C} \left(\sum_{n=0}^C \binom{C}{n} G_1^n G_0^{C-n} \frac{1}{2^{C-n}} (Q_1^n + (1-Q_1)^n) h_n - h \left(\frac{Q_\mu^C}{Q_\mu^C + (1-Q_\mu)^C} \right) \right) \quad (57)$$

Note that this expression can only be higher than the one derived in [11] which only took into account rounds where *all* C rounds had single photons. Our new proof methodology is able to determine the entropy in all rounds where Alice does not send two or more photons in a block. Of course, the above depends on both observable quantities, such as G_μ and Q_μ , and also unobservable quantities, such as Q_1 , G_0 , and G_1 . However, these unobservable quantities can be bounded using the decoy state method, as we discuss next.

Note that the above analysis assumed collective attacks; however since the protocol is permutation invariant, standard post selection or de Finetti style arguments may be made to promote the analysis to general attacks [24, 25, 26] (these methods also apply to CAD [10, 11]).

3.3 Decoy State Analysis

Now, the above expression depends on several observable quantities, such as G_μ and Q_μ ; however it also depends on several unobservable quantities, such as G_1 , G_0 , and Q_1 . However, these unobservable quantities can be readily estimated using the decoy state method [6, 7, 8]. In particular, assume signal qubits (those which will contribute to the raw key) are emitted using a power level of μ . Let $p_n = p(n|\mu) = e^{-\mu} \mu^n / n!$ be the probability Alice's source emits n photons on any given round assuming she set her power level to μ . Recall that $G_n = p(n|acc)$, the probability that Alice sent n photons initially, conditioned on Bob distilling a raw key bit (i.e., conditioned on parties accepting a particular round). Using Bayes' theorem, we can write $G_n = p(n|acc) = p(acc|n)p_n/p(acc)$. Here, $p(acc) = G_\mu$ is simply the total probability of accepting any particular round before CAD (i.e., a quantum communication stage round, *not* a CAD block - we are currently looking at statistics before CAD is run). Let $Y_n = p(acc|n)$ be the n -photon yield, then we have:

$$p(acc) = G_\mu = \sum_{n \geq 0} p_n Y_n. \quad (58)$$

Let's next investigate the error terms Q_n and Q_μ . The latter, is the averaged observed error which is simply:

$$Q_\mu = \sum_{n \geq 0} G_n Q_n = \sum_{n \geq 0} \frac{p_n Y_n}{G_\mu} Q_n. \quad (59)$$

We also require Q_n , the probability of a Z basis error conditioned on Alice initially sending n photons and parties accepting this round of the quantum communication stage. Of course, $Q_0 = 1/2$, as discussed earlier, while the decoy state method can be used to bound Q_n , for $n \geq 1$. We consider two versions of the decoy state method, below: the infinite decoy method and the two decoy method. Others are possible (see, for instance, [18]), and our entropy analysis can be applied to those as well.

Infinite Decoy State Analysis: In the infinite decoy state method, where Alice may choose from an infinite number of decoy levels μ , Alice and Bob may directly estimate Y_n (and thus G_n and Q_n), by setting up a suitable system of equations (see, for instance, [8]). One would expect (and can even

enforce under such conditions) a standard optical QKD implementation to obey statistics shown in Table 1 (derived from [18], using our notation). These values, in our simulations later, will depend on several device parameters, including p_{dark} , the dark count rate, f , the efficiency of the detectors, and e_{det} , the probability a photon hits the wrong detector. We also need to consider the overall transmittivity of the channel, which is taken to be $\eta = 10^{-\alpha d/10} f$, where d is the total distance between parties, and α is the loss coefficient which, later, we set to $\alpha = 0.21$ to be consistent with [11].

Table 1: Notation for decoy state parameters and observables, along with expected experimental values, from [18, 11]. Here, G_μ and Q_μ are observable quantities. The decoy state method allows for Alice and Bob to determine bounds on G_n and Q_n which are typically not directly observable.

Symbol	Description	Expected Experimental Value
f	Detector efficiency	
d	Distance between parties	
α	Loss coefficient	
p_{dark}	Dark count probability	
e_{det}	Probability a photon hits the wrong detector	
η	Total transmission probability of a photon	$f \cdot 10^{-\alpha d/10}$
η_n	Transmittance of an n photon state	$1 - (1 - \eta)^n$
p_n	Probability of sending n photons	$\exp(-\mu)\mu^n/n!$
Y_0	Yield of vacuum round	p_{dark}
Y_n	Yield of n photon round	$\eta_n + (1 - \eta_n)p_{dark} \approx \eta_n + p_{dark}$
G_μ	Total Gain ($\sum_{n \geq 0} p_n Y_n$)	$Y_0 + (1 - \exp(-\eta\mu))$
G_n	Gain of n photon round	$\frac{Y_n p_n}{G_\mu}$
Q_0	Bit error rate of vacuum round	$\frac{1}{2}$
Q_n	Bit error rate of n photon round	$\frac{Q_0 Y_0 + e_{det} \eta_n}{Y_n}$
Q_μ	Average observed error	$\frac{Q_0 Y_0 + e_{det} (1 - \exp(-\eta\mu))}{G_\mu}$

Two Decoy State Analysis: Having infinite decoy states to choose from is suitable for an asymptotic analysis; however in practice, one typically chooses from a finite number of power levels. We next consider the two-decoy method, using bounds derived in [18].

For the two decoy method, μ will remain our chosen signal state power level, however two other power levels will be chosen, ν_1 and ν_2 , subject to the constraint $\nu_1 + \nu_2 < \mu$ and $0 < \nu_2 < \nu_1$. In general, ν_2 will be set close to zero, essentially “shutting off” Alice’s source device on those rounds, thus allowing parties to get highly accurate statistics on Y_0 .

Parties run the QKD protocol, allowing them to observe G_μ and Q_μ as before, but also G_{ν_i} and Q_{ν_i} , which are defined similarly to G_μ and Q_μ , however, now, they are the average whenever Alice chooses power level ν_i . Using these, parties determine the following lower-bounds on Y_0 and Y_1 (see [18] for details on these derivations):

$$Y_0 \geq Y_0^L = \frac{\nu_1 G_{\nu_2} e^{\nu_2} - \nu_2 G_{\nu_1} e^{\nu_1}}{\nu_1 - \nu_2} \quad (60)$$

$$Y_1 \geq Y_1^L = \frac{\mu}{\mu(\nu_1 - \nu_2) - \nu_1^2 + \nu_2^2} \left(G_{\nu_1} e^{\nu_1} - G_{\nu_2} e^{\nu_2} - \frac{\nu_1^2 - \nu_2^2}{\mu^2} (G_\mu e^\mu - Y_0^L) \right) \quad (61)$$

The above allows parties to determine bounds on G_0 and G_1 (recall, $G_n = Y_n p_n / G_\mu$), needed to evaluate our key-rate expression.

What remains is to determine an upper-bound bound on Q_1 (which will produce a lower-bound on the key-rate). However, again using results from [18], this is found to be:

$$Q_1 \leq Q_1^U = \frac{G_{\nu_1} Q_{\nu_1} e^{\nu_1} - G_{\nu_2} Q_{\nu_2} e^{\nu_2}}{(\nu_1 - \nu_2) Y_1^L} \quad (62)$$

This provides us with everything we need to evaluate Equation 57. Note that the error correction leakage (the $H(K|B)$ term in our security proof) remains a function of Q_μ as we are assuming raw key bits are distilled through rounds where Alice chose μ as her power level.

3.4 Comment on Finite Key Security

For finite key security, one requires a bound on the *smooth quantum min entropy*, $H_\infty^\epsilon(K|EM)$, defined in [20]. However, assuming collective attacks, one can bound the min entropy using the von Neumann entropy (i.e., using our bound in Theorem 2), and subtracting a suitable error term. In particular, for states of the form $\rho_{KEM}^{\otimes n}$, one may use the quantum asymptotic equipartition property (AEP) [27] to bound the smooth min entropy as:

$$\frac{1}{n} H_\infty^\epsilon(K|EM) \geq H(K|EM) - \frac{4}{\sqrt{n}} \log_2(2 + \sqrt{2}) \sqrt{\log_2 \frac{2}{\epsilon^2}}. \quad (63)$$

where n , above, is the size of the raw key (after CAD is run; i.e., $n = |K|$ where K is the new key register after CAD). One can also promote this to general attacks using post-selection methods [25], however, this adds an additional error term of $30 \log_2(n' + 1)/n'$ (see [28] for details), where n' is the total number of signals received by Bob before CAD is run (including those which will be used for testing, as we are no longer able to bias the signal state choice and Z basis choice arbitrarily close to one, as we did in the asymptotic case). Finally, one must also take into account imperfect sampling effects and derive suitable confidence intervals for any observed statistic. However, these confidence intervals can be found through standard techniques (see, for instance, [29]).

The above are standard techniques for promoting asymptotic proofs of security to finite key ones. This gives a complete security proof, however one which, *in the finite key scenario*, is sub-optimal due to the additional error terms induced by applying these approximation methods. Note that this was the method employed in prior work in [11] and so any “gap” between our results and results from [11] in the asymptotic scenario (shown in Section 4), would remain exactly the same in the finite key setting using these methods. Thus, we do not perform this comparison in this work, as it would not be interesting.

We comment that a finite key result was proven in [19] by bounding the min entropy directly; however that result used a different CAD process which was claimed to be insecure on blocks with vacuum rounds. Furthermore, in [16], a direct min entropy proof was developed for CAD applied to a conference key agreement protocol, though only for CAD blocks of size two (i.e., $C = 2$) and single photon sources. It would be interesting to see if a direct min entropy bound can be derived for the CAD protocol we consider here (which is a more standard CAD process and which, we proved here, does have non-zero entropy in blocks with vacuum rounds). Perhaps methods developed in [19, 16] can be used towards this end, though we leave this as future work. This paper was interested in exploring the potential benefit of a complete CAD analysis for the decoy state

protocol (by complete, we mean taking advantage of all possible blocks which may lead to non-zero entropy). Computing an optimal finite key bound is out of scope for this paper.

4 Evaluation

We compare our asymptotic key-rate bound, Equation 57, to that derived in [11]. This is, to our knowledge, the state of the art for this particular CAD protocol in the asymptotic setting, so will give us the “highest bar” to compare to.

We first compare the two key-rate results, assuming the infinite decoy state method, whereby users will gain complete confidence in each of the required, individual, statistics G_0 , G_1 and Q_1 (note that G_0 is not required for prior work in [11] as they only considered single-photon events). In this case, using statistics from Table 1, we plot the resulting key-rates in Figure 1 for $f = 0.04$ (i.e., a low detector efficiency of 4%), $e_{det} = 0.05$, and using a signal power level of $\mu = 0.48$ (which is the setting used in [11]). We note for high distances, our result always outperforms prior work, allowing for increased QKD distances. For lower distances (Figure 1 Right). Our work matches prior work, and there is no advantage (nor is there any disadvantage) to considering vacuum rounds. Of course, in low distances, as shown in Figure 1 Right, it is not advantageous to use CAD as the loss in key-rate due to CAD compression outweighs any benefits gained. However, since the decision to use CAD can be performed after observing the channel noise, parties may make an advantageous decision after running the quantum communication stage, as to whether or not to use CAD, and what block level C to use.

In Figure 2, we consider the effect of noise on the performance of the system, comparing to prior work. We use the same detector settings as before, but now fix d (the distance between parties), to be 50km (Figure 2 Left) and 170km (Figure 2 Right). We note that at small distances, there is no advantage to our result (though, also, no disadvantage, as the result matches prior work); however at higher distances, there can be a large advantage in noise tolerance when using our result.

We perform the same tests for the six-state BB84 in Figure 3. As expected, longer distances, and higher noise tolerances are possible for this protocol; again we see our work outperforms prior work, for long distances, and high noise, channels.

Finally, we also evaluate the two decoy state protocol in Figures 4 (for the two-basis version), and 5 (for the three-basis, six-state, version). We note that the more practical two-decoy protocol does not perform as well as the infinite version, as expected, however we also note that our work again outperforms prior work.

Ultimatley, our evaluations show that our new key-rate bound can outperform prior work in high distances and high noise scenarios; however it also never “underperforms” when compared to prior CAD work (in fact, it is straight-forward to prove using basic properties of von Neumann entropy, that our result can never be lower than prior work in [11]). While the improvement produced by our key-rate compared to CAD results in [11], is not as substantial as the improvement shown in [11] when comparing to results *without CAD*, our work still does allow for increased distances, and increased noise tolerances, as our evaluations show. Our work also “completes the proof” in a sense, by considering all possible events that can lead to non-zero uncertainty for Eve in a CAD block.

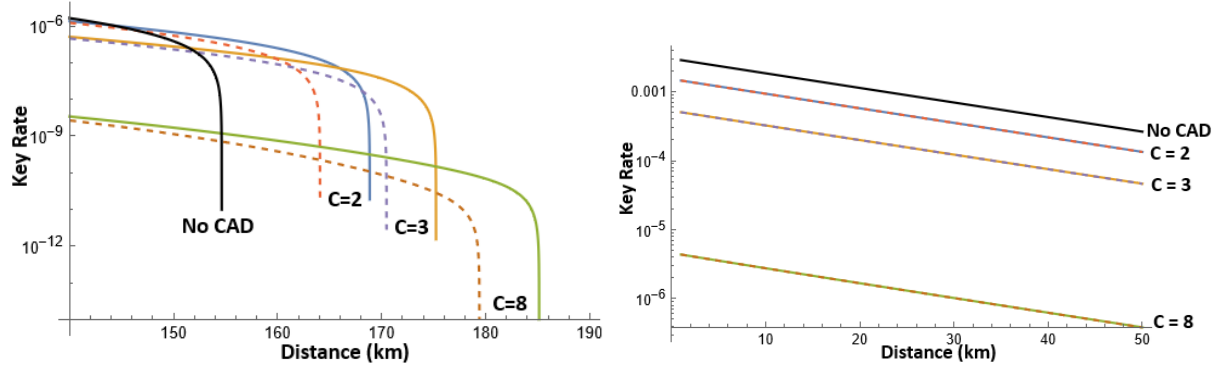


Figure 1: Comparing our new result (Solid lines, Equation 57) with prior work in [11] (Dashed lines) for the four-state BB84 protocol using infinite decoy states. We test a CAD block size of $C = 2$ (Blue/Red), $C = 3$ (Yellow/Purple), and $C = 8$ (Green/Orange). We note that in all cases, our result outperforms prior work, allowing for increased distances. Here we set $e_{det} = 0.05$, $p_d = 10^{-6}$, and $f = .04$. We also use $\mu = 0.48$. A comparison to the case without CAD is also shown (Black Solid line). Right: Similar to the left graph, but showing smaller distances ranging from 1 to 50km. Here we note that there is no difference in our result and prior work; furthermore, we note that CAD actually hinders performance. Thus CAD should only be utilized at suitably high distances.

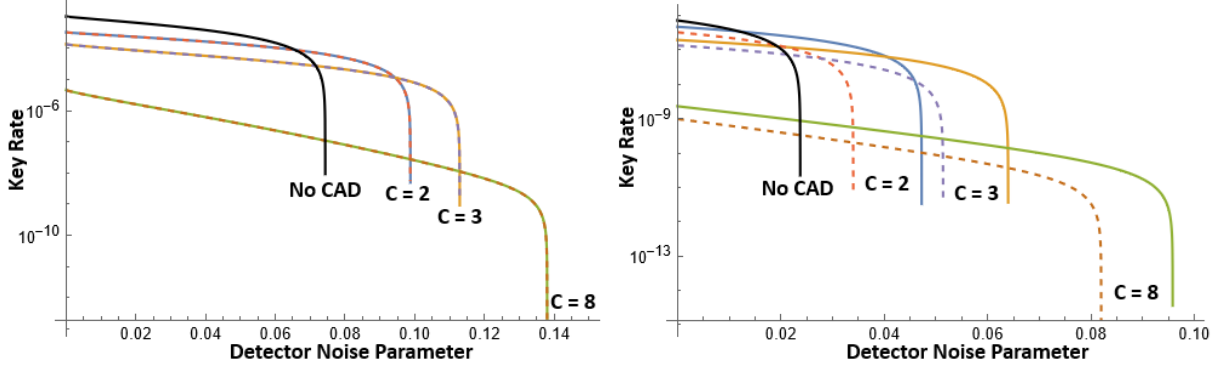


Figure 2: Comparing key-rate between our new result (solid) and prior work (dashed) as noise increases for a fixed distance of $d = 50\text{km}$ (Left) and $d = 170\text{km}$ (Right). We see that at high distances, our result outperforms prior work, including standard decoy state results without CAD, allowing for increased noise tolerance. At lower distances, our work is numerically equivalent to prior work.

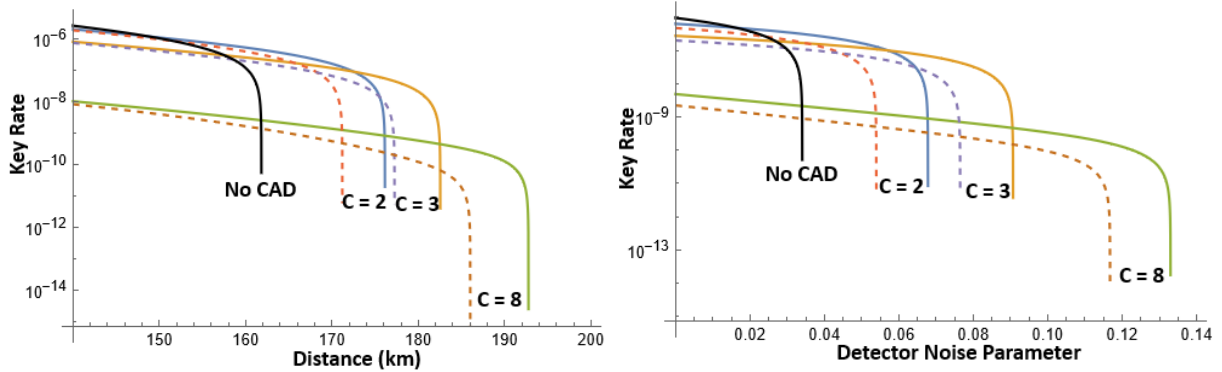


Figure 3: Comparing our work (solid lines) with prior work (dashed lines) for the six state decoy BB84 protocol. Left: We fix $e_{det} = 0.05$ and vary the distance; Right: We fix the distance at $d = 170\text{km}$ and vary the noise e_{det} . Note that in all cases, our work outperforms prior work. We also note that CAD can substantially improve decoy state performance, as originally observed in [11]. Not surprisingly, six-state BB84 outperforms the four state version.

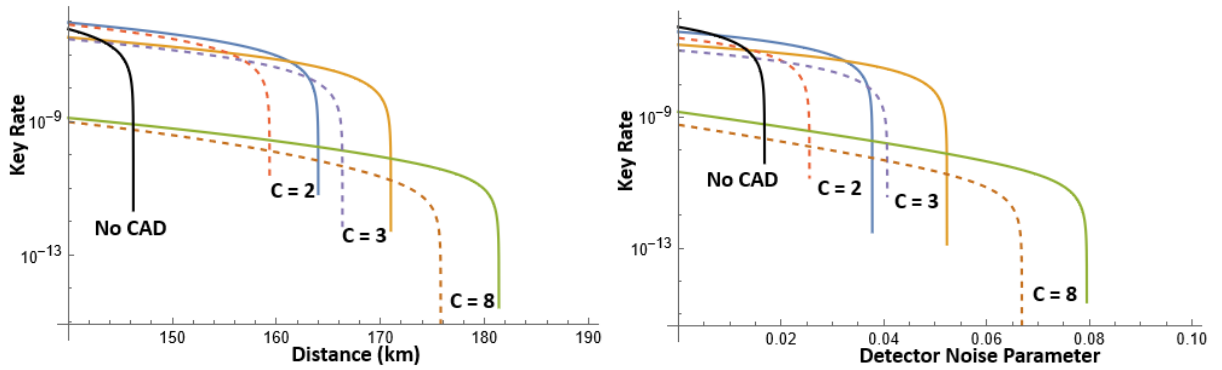


Figure 4: Comparing our work (solid lines) with prior work (dashed lines) for the two-decoy BB84 protocol. Left: We fix $e_{det} = 0.05$ and vary the distance; Right: We fix the distance at $d = 170\text{km}$ and vary the noise e_{det} . As expected, the two-decoy protocol does not perform as well, asymptotically, as the infinite decoy version, however the difference is not very substantial; we also note that, as before, our work produces better results.

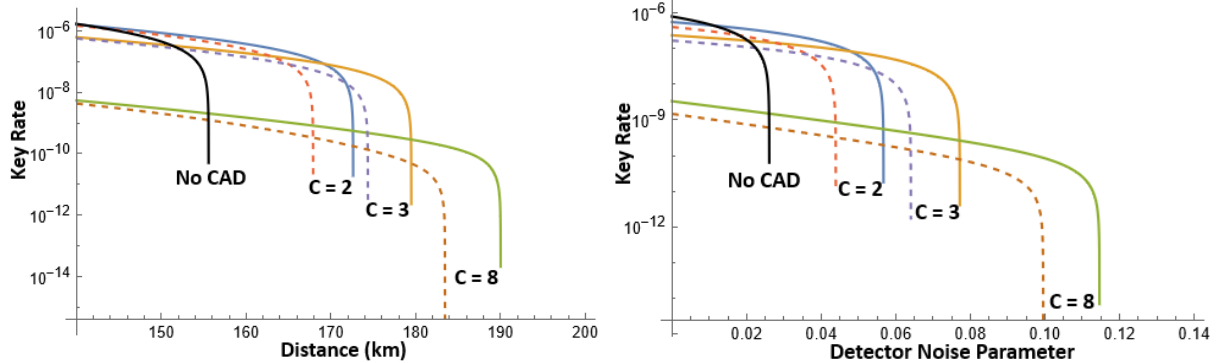


Figure 5: Comparing our work (solid lines) with prior work (dashed lines) for the two-decoy, six-state, BB84 protocol. Left: We fix $e_{det} = 0.05$ and vary the distance; Right: We fix the distance at $d = 170\text{km}$ and vary the noise e_{det} .

5 Closing Remarks

In this paper, we derived a new proof of security for CAD applied to the decoy-state BB84 protocol in the asymptotic setting (though, as discussed in Section 3.4, our work can also be used in the finite key setting). In [11], it was shown that CAD can greatly benefit the decoy-state BB84 protocol’s performance. However all prior work, to our knowledge, only considered blocks of single-photon rounds, thus providing a correct, though sub-optimal bound on the overall key-rate. Our proof in this paper, is able to derive a non-trivial entropy bound for all possible cases of single and vacuum photon rounds in a CAD block. Due to this, our work outperformed prior work and showed that CAD can further improve BB84 performance when using practical devices. Since multi-photon rounds in a CAD block leak full information to an adversary, our proof is, in a sense, complete.

There are many interesting open problems. Perhaps the most important is deriving a tight finite key proof of security. While our work, as discussed in Section 3.4, can be used in the finite key setting, it would require the use of approximation methods to use our Theorem 2 to bound the quantum min entropy, needed to derive a finite key bound. These approximation methods will produce a correct, however a sub-optimal result. Finding methods to bound the min entropy directly is an important research area. Perhaps by adopting methods from [19] (which involved a different CAD protocol), and [16] (which considered conference key agreement), combined with techniques we developed here, will prove fruitful.

Another interesting future direction would be to apply our proof method to other QKD protocols, beyond BB84. For instance, in [11], a measurement device independent (MDI) protocol was considered, but again only blocks consisting of all single photon rounds were considered. Our methods may be applicable there to improve the overall key-rate of MDI-QKD with CAD. Alternatively, looking at CAD and twin-field protocols, as was done in [13, 14, 15], could be interesting, and perhaps our methods may be helpful in improving key-rates for this class of QKD protocol also; though we leave that investigation as future work.

Acknowledgments: WOK would like to acknowledge support from the NSF under grant number 2143644

References

- [1] Stefano Pirandola, Ulrik L Andersen, Leonardo Banchi, Mario Berta, Darius Bunandar, Roger Colbeck, Dirk Englund, Tobias Gehring, Cosmo Lupo, Carlo Ottaviani, et al. Advances in quantum cryptography. *Advances in optics and photonics*, 12(4):1012–1236, 2020.
- [2] Charles H Bennett and Gilles Brassard. Quantum cryptography: Public key distribution and coin tossing. In *Proceedings of IEEE International Conference on Computers, Systems and Signal Processing*, volume 175. New York, 1984.
- [3] Gilles Brassard, Norbert Lütkenhaus, Tal Mor, and Barry C Sanders. Limitations on practical quantum cryptography. *Physical review letters*, 85(6):1330, 2000.
- [4] Gilles Brassard, Norbert Lütkenhaus, Tal Mor, and Barry C Sanders. Security aspects of practical quantum cryptography. In *International conference on the theory and applications of cryptographic techniques*, pages 289–299. Springer, 2000.
- [5] Daniel Gottesman, Hoi-Kwong Lo, Norbert Lütkenhaus, and John Preskill. Security of quantum key distribution with imperfect devices. *Quantum Info. Comput.*, 4(5):325–360, September 2004.
- [6] Won-Young Hwang. Quantum key distribution with high loss: toward global secure communication. *Physical review letters*, 91(5):057901, 2003.
- [7] Xiang-Bin Wang. Beating the photon-number-splitting attack in practical quantum cryptography. *Physical review letters*, 94(23):230503, 2005.
- [8] Hoi-Kwong Lo, Xiongfeng Ma, and Kai Chen. Decoy state quantum key distribution. *Physical review letters*, 94(23):230504, 2005.
- [9] Ueli M Maurer. Secret key agreement by public discussion from common information. *IEEE transactions on information theory*, 39(3):733–742, 2002.
- [10] Joonwoo Bae and Antonio Acín. Key distillation from quantum channels using two-way communication protocols. *Physical Review A—Atomic, Molecular, and Optical Physics*, 75(1):012334, 2007.
- [11] Hong-Wei Li, Chun-Mei Zhang, Mu-Sheng Jiang, and Qing-Yu Cai. Improving the performance of practical decoy-state quantum key distribution with advantage distillation technology. *Communications Physics*, 5(1):53, 2022.
- [12] Li Gong, Chenpeng Hao, Zhijiang Chen, Yang Wang, Xiangqun Fu, Jianhong Shi, Chun Zhou, and Hongwei Li. Experimental demonstration of decoy-three-state quantum key distribution with advantage distillation. *Optics Letters*, 50(21):6807–6810, 2025.
- [13] Yao Zhou, Rui-Qiang Wang, Chun-Mei Zhang, Zhen-Qiang Yin, Ze-Hao Wang, Shuang Wang, Wei Chen, Guang-Can Guo, and Zheng-Fu Han. Sending-or-not-sending twin-field quantum key distribution with advantage distillation. *Physical Review Applied*, 21(1):014036, 2024.

- [14] Chun-Mei Zhang, Zhe Wang, Yu-Da Wu, Jian-Rong Zhu, Rong Wang, and Hong-Wei Li. Discrete-phase-randomized twin-field quantum key distribution with advantage distillation. *Physical Review A*, 109(5):052432, 2024.
- [15] Hong-Wei Li, Rui-Qiang Wang, Chun-Mei Zhang, and Qing-Yu Cai. Improving the performance of twin-field quantum key distribution with advantage distillation technology. *Quantum*, 7:1201, 2023.
- [16] Walter O Krawec. Quantum conference key agreement with classical advantage distillation. *Discover Networks*, 1(1):5, 2025.
- [17] Rui-Qiang Wang, Chun-Mei Zhang, Zhen-Qiang Yin, Hong-Wei Li, Shuang Wang, Wei Chen, Guang-Can Guo, and Zheng-Fu Han. Phase-matching quantum key distribution with advantage distillation. *New Journal of Physics*, 24(7):073049, 2022.
- [18] Xiongfeng Ma, Bing Qi, Yi Zhao, and Hoi-Kwong Lo. Practical decoy state for quantum key distribution. *Physical Review A—Atomic, Molecular, and Optical Physics*, 72(1):012326, 2005.
- [19] Jonas Treplin, Philipp Kleinpaß, and Davide Orsucci. Finite size analysis of decoy-state bb84 with advantage distillation. *arXiv preprint arXiv:2511.21665*, 2025.
- [20] Renato Renner. Security of quantum key distribution. *International Journal of Quantum Information*, 6(01):1–127, 2008.
- [21] Igor Devetak and Andreas Winter. Distillation of secret key and entanglement from quantum states. *Proceedings of the Royal Society A: Mathematical, Physical and engineering sciences*, 461(2053):207–235, 2005.
- [22] Walter O Krawec. Quantum key distribution with mismatched measurements over arbitrary channels. *Quantum Information & Computation*, 17(3-4):209–241, 2017.
- [23] Barbara Kraus, Nicolas Gisin, and Renato Renner. Lower and upper bounds on the secret-key rate for quantum key distribution protocols using one-way classical communication. *Physical review letters*, 95(8):080501, 2005.
- [24] Renato Renner, Nicolas Gisin, and Barbara Kraus. Information-theoretic security proof for quantum-key-distribution protocols. *Physical Review A—Atomic, Molecular, and Optical Physics*, 72(1):012332, 2005.
- [25] Matthias Christandl, Robert König, and Renato Renner. Postselection technique for quantum channels with applications to quantum cryptography. *Physical review letters*, 102(2):020504, 2009.
- [26] Renato Renner. Symmetry of large physical systems implies independence of subsystems. *Nature Physics*, 3(9):645–649, 2007.
- [27] Marco Tomamichel, Roger Colbeck, and Renato Renner. A fully quantum asymptotic equipartition property. *IEEE Transactions on information theory*, 55(12):5840–5847, 2009.
- [28] Lana Sheridan, Thinh Phuc Le, and Valerio Scarani. Finite-key security against coherent attacks in quantum key distribution. *New Journal of Physics*, 12(12):123019, 2010.

[29] Marco Tomamichel, Charles Ci Wen Lim, Nicolas Gisin, and Renato Renner. Tight finite-key analysis for quantum cryptography. *Nature communications*, 3(1):634, 2012.